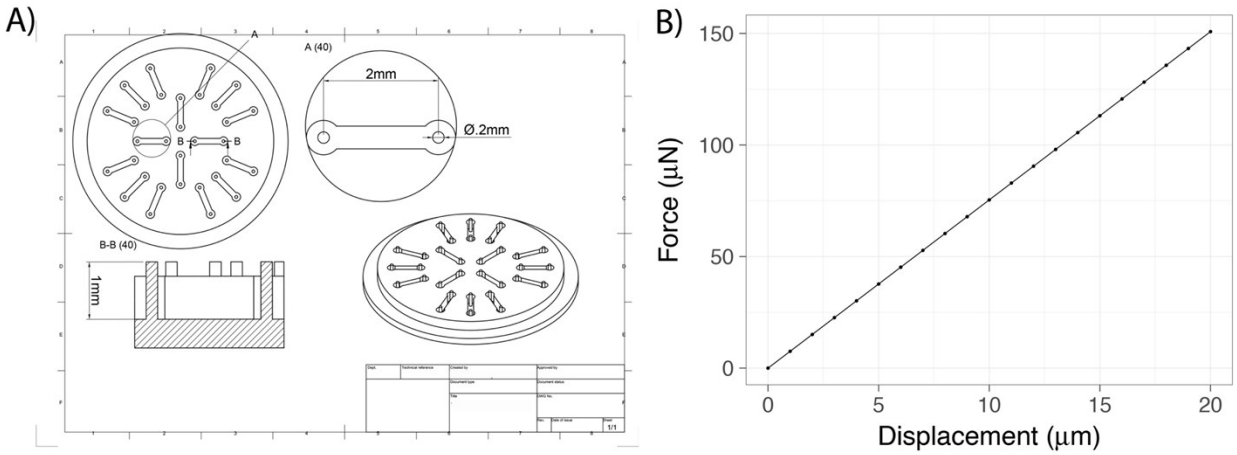

Figure S1: A) Layout of the microposts within one well. 16 individual sets of microposts are arranged within one well. Each set of microposts is spaced 2 mm apart from post center to opposing post center, and each individual micropost has a diameter of 200 µm and a length of 1 mm. Each individual "dog bone" set of microposts is seeded with one clot so that up to 16 independent deflection measurements can be taken within each well. In practice, 5-6 seeded sets of microposts from each well were used during each experiment, and 3 independent experiments were conducted for a total n = 16/group. B) Force vs. displacement curve for micropost deflection model, developed based on the micropost geometry and modulus. The curve is modeled by the equation $F = 7.5\delta$, in which F represents force generated and δ represents displacement.

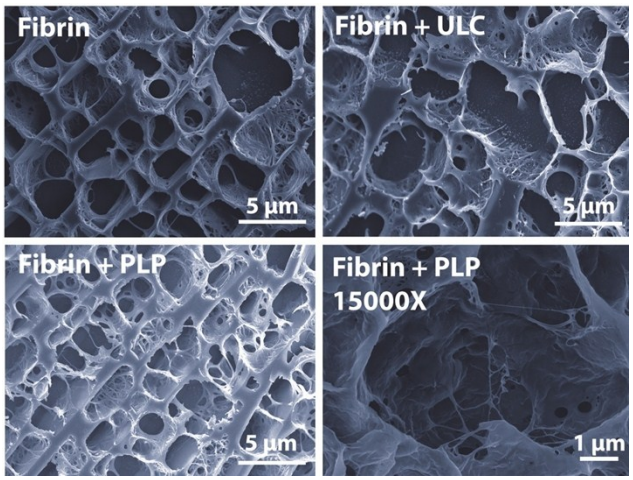

Figure S2: The ability of PLPs to induce clot retraction when incorporated into fibrin clots was evaluated using cryoSEM. Clots comprised of 2 mg/ml human fibrinogen and 0.1 U/ml human α-thrombin were imaged 24 hours after polymerization. ULC- and PLP-incorporated clots contained 0.5 mg/ml ULCs or PLPs. All images were taken at 5000X magnification with the exception of the bottom right fibrin + PLP image, which was taken at 15000X. Control fibrin clots display less dense network structure than fibrin + PLP clots, whereas fibrin + ULC clots display less dense network structure than control fibrin clots. At 15000X magnification, PLPs can be seen interacting with fibrin fibers within the network. n = 3 clots/group, 3 images/clot; representative images are shown.

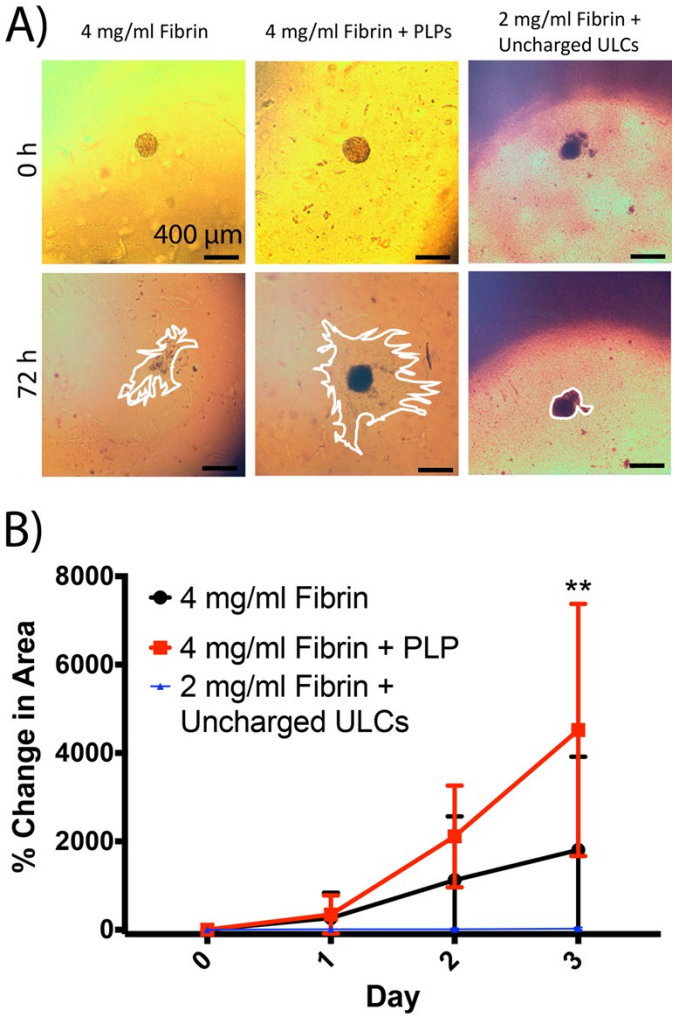

Figure S3: Fibroblast migration outward from spheroids embedded in fibrin matrices in the presence and absence of PLPs (0.5 mg/ml) in matrices comprised of 4 mg/ml fibrinogen or in the presence of uncharged ULCs in matrices comprised of 2 mg/ml fibrinogen and uncharged ULCs (0.5 mg/ml). Migration is significantly increased in the presence of PLPs in 4 mg/ml fibrinogen matrices and is very limited in the presence of uncharged ULCs compared to fibrin only controls. Representative brightfield images of the spheroids at 0 and 72 hour time points (A) and mean spheroid area ± standard deviation for each time point (B) are shown. **: $p < 0.01$. n = 5/group

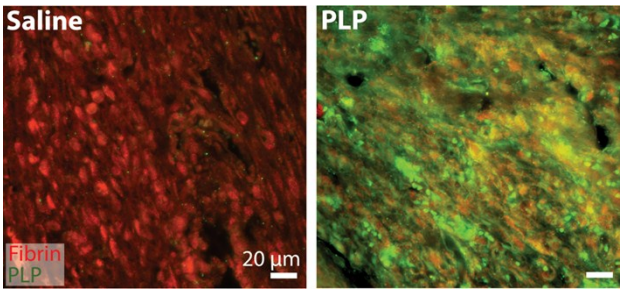

Figure S4: Immunohistochemistry of fibrin and PLP colocalization throughout wound tissue collected 9 days post injury. PLP-treated wounds demonstrate extensive integration of PLPs (green) throughout the fibrin network (red).

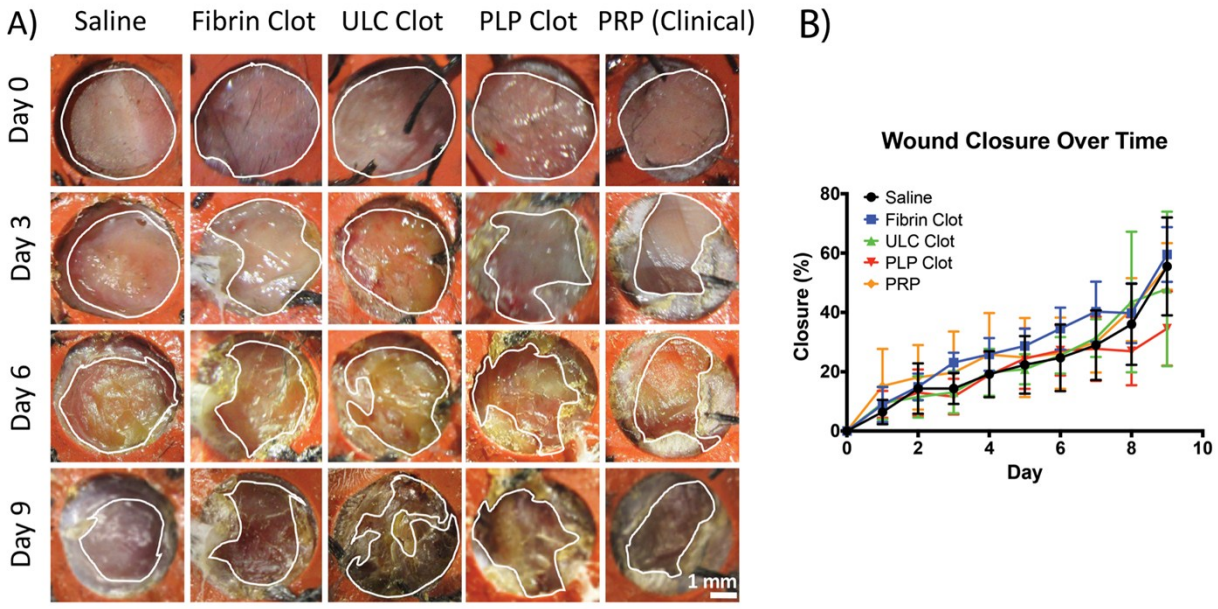

Figure S5: Wound closure over time for wounds treated with saline, PRP, or fibrin formed in the absence or presence of ULC microgels or PLPs. Fibrin clots were made at concentrations of 2 mg/ml human fibrinogen and 0.1 U/ml human α-thrombin. ULCs or PLPs were incorporated into clots at 0.5 mg/ml. Fibrin clots were then applied topically to wounds and allowed to polymerize for 1 hour prior to application of wound dressings. Wounds were imaged daily for 9 days. Representative wound images over time are shown; outlines of the wound boundaries are shown

in white. Percent wound closure was calculated and mean percent closure values over time ± standard deviation are presented. n = 5 wounds/group.